Investigation of Wave Height Reduction behind the Wave Dragon Wave Energy Converters and Application in Santander, Spain

Nørgaard, Jørgen Quvang Harck; Andersen, Thomas Lykke

Publication date:
2015

Document Version
Publisher's PDF, also known as Version of record

DEPARTMENT OF CIVIL ENGINEERING
AALBORG UNIVERSITY

Investigation of Wave Height Reduction behind the Wave Dragon Wave Energy Converters and Application in Santander, Spain

Jørgen Quvang Harck Nørgaard
Thomas Lykke Andersen

ISSN 1901-726X
DCE Technical Report No. 203

Aalborg University
Department of Civil Engineering
Group Name

DCE Technical Report No. 203

Investigation of Wave Height Reduction behind the Wave Dragon Wave Energy Converters and Application in Santander, Spain

by

Jørgen Quvang Harck Nørgaard
Thomas Lykke Andersen

June 2015

Scientific Publications at the Department of Civil Engineering

Technical Reports are published for timely dissemination of research results and scientific work carried out at the Department of Civil Engineering (DCE) at Aalborg University. This medium allows publication of more detailed explanations and results than typically allowed in scientific journals.

Technical Memoranda are produced to enable the preliminary dissemination of scientific work by the personnel of the DCE where such release is deemed to be appropriate. Documents of this kind may be incomplete or temporary versions of papers—or part of continuing work. This should be kept in mind when references are given to publications of this kind.

Contract Reports are produced to report scientific work carried out under contract. Publications of this kind contain confidential matter and are reserved for the sponsors and the DCE. Therefore, Contract Reports are generally not available for public circulation.

Lecture Notes contain material produced by the lecturers at the DCE for educational purposes. This may be scientific notes, lecture books, example problems or manuals for laboratory work, or computer programs developed at the DCE.

Theses are monograms or collections of papers published to report the scientific work carried out at the DCE to obtain a degree as either PhD or Doctor of Technology. The thesis is publicly available after the defence of the degree.

Latest News is published to enable rapid communication of information about scientific work carried out at the DCE. This includes the status of research projects, developments in the laboratories, information about collaborative work and recent research results.

Published 2015 by
Aalborg University
Department of Civil Engineering
Sofiendalsvej 9-11
DK-9200 Aalborg SV, Denmark

Printed in Aalborg at Aalborg University

ISSN 1901-726X
DCE Technical Report No. 203

Investigation of Wave Height Reduction behind the Wave Dragon Wave Energy Converters and Application in Santander, Spain

Jørgen Quvang Harck Nørgaard[1] and Thomas Lykke Andersen[1]

This paper deals with a case study on the wave height reduction behind floating Wave Dragon wave energy converters in Santander Bay, Spain. The study is performed using the MIKE21 Boussinesq model from DHI. The Wave Dragon transmission characteristics in the numerical wave propagation model are based on previously performed physical model tests in scale 1:51. Typical winter storm conditions are considered in the case study together with different stiffness in the mooring system of the floating device. From the study it is found that if multiple Wave Dragons are positioned in a farm the wave power along the shorelines in Santander Bay is reduced by approximately 50% when using the farm layout of that provides the best overall compromise between coastal protection and electricity production. Moreover, it is concluded that a farm of devices can be modelled with good accuracy using a homogeneous porosity structure instead of implementing each device with detailed geometry.

1. INTRODUCTION

Significant costs are related to production of electricity from offshore Wave Energy Converters (WECs). An innovative idea is to use WECs for protection of coastlines and thereby share the costs between electricity production and coastal protection. Such approach is studied in the European THESEUS project (THESEUS, 2012), which has supported the present study.

Numerical wave propagation models are seen to be powerful tools when evaluating the wake of offshore WECs such as in the studies by: Smith (2007), Venugopal & Smith (2007), Beels et al. (2010), Palha et al. (2010), and Roul P. et al. (2011). The models can be used to analyze the effects of a WEC-farm at a specific bathymetry and in the specific wave conditions.

A shortcoming in the previous mentioned studies is, however, that the numerical models have not been calibrated or validated against the actual measured wave pattern behind the considered devices. Moreover, the influences of the heave, surge, and pitch movements of the floating WECs are typically neglected.

The objective of the present paper is to obtain a realistic estimate of the wave height reduction behind offshore floating Wave Dragon (WD) WECs in Santander Bay, Spain, using a numerical wave propagation model, which is calibrated against physical model tests. Additionally, the objective is to evaluate simplified methods for implementation of floating WECs in wave propagation models.

2. CONTENTS OF THE PAPER

Initially, the considered WD is presented. This is followed by a brief presentation of the findings from the previous studies by Nørgaard et al. (2011) and Nørgaard & Lykke Andersen (2012) on physical model tests and calibration of a 2-D depth integrated Boussinesq model, respectively. The calibrated numerical model by Nørgaard & Andersen (2012) is used in the present paper for determining the overall wave transmission coefficient of a farm of floating WDs. Finally, a detailed analysis is performed on the wave height reduction in Santander Bay, Spain, and a simplified implementation of the WDs in MIKE21 BW is evaluated.

[1] Department of Civil Engineering, Aalborg University, Sohngaardsholmsvej 57, DK-9000, Denmark, jhn@civil.aau.dk, tla@civil.aau.dk,

3. THE WAVE DRAGON DEVICE

The considered WD-device in this paper is the 260 *x* 150 *m* 24 *kW/m* WD-model, illustrated in Figure 1. The WD consists of two main elements: two wave reflectors and a main body. The reflectors focus the waves towards a reservoir above mean sea level and electricity is produced when the water in the reservoir drains through turbines. The floating device is moored and is able to turn and face the incident wave direction. An advanced pneumatic system is used to adjust the floating level and thereby optimize the rate of wave overtopping and electricity production.

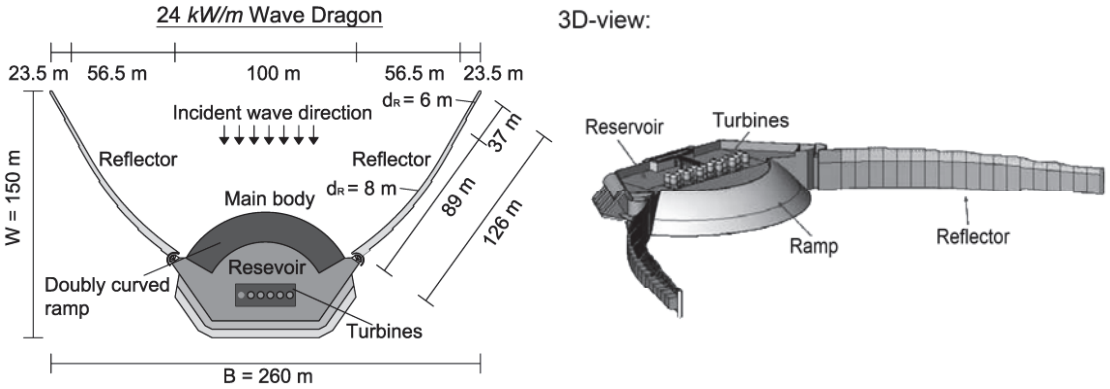

FIGURE 1. ***(left)*** **Illustration and dimensions of the considered prototype WD-model (Nørgaard et al., 2011).** ***(right)*** **3-D illustration of the floating WD (Tedd, 2007).**

3.1 RESTRICTIONS FOR WD-POSITIONING IN A FARM

Offshore wave energy converters are typically positioned in farms to reduce the costs related to moorings and power cables. According to Beels et al. (2010) a minimum individual lateral distance of $1 \cdot B$ = 260 *m* should be used when positioning multiple WDs in a farm to prevent collision in the case where one WD is fixed in its far position due to a fault, and its neighboring WD turn to the other far position. The rotation of the WD is assumed to be restricted to a rotation of $\pm 60^{o}$ by its mooring system, (Beels et al., 2010), illustrated in Figure 2 (*left*). To avoid collisions in the case where the WDs are placed in a staggered pattern, a minimum longitudinal distance of 340 *m* should be used between the reflector-tip's, as illustrated in Figure 2 (*right*).

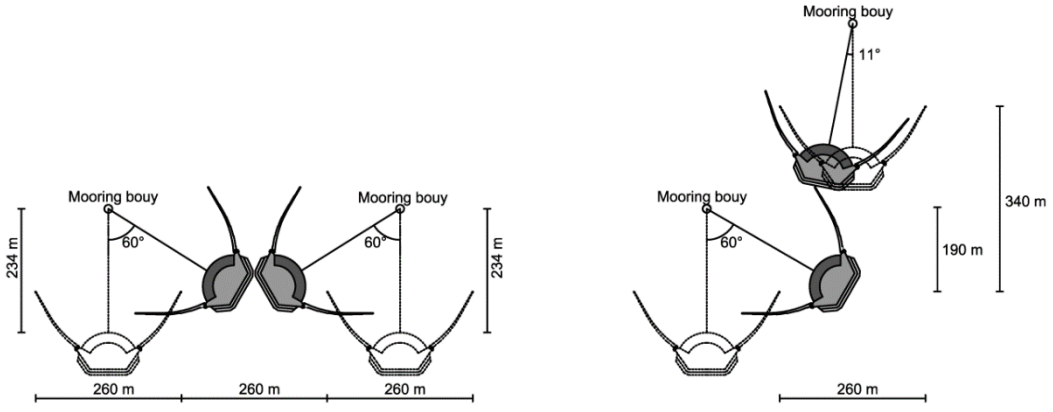

Figure 2. (*left*) Lateral distance between WDs in a farm. (*right*) Longitudinal distance between individual WDs in a staggered grid. (Nørgaard et al., 2011).

4. Previous Physical Model Tests on Wave Disturbances behind a Single WD-device

In the physical tests by Nørgaard et al. (2011) the wave disturbance coefficient was measured from wave gauges at various positions behind the WD-device. The wave disturbance coefficients were defined by $K_d = H_{s,measured}/H_{s,i}$, where $H_{s,measured}$ is the measured significant wave height in the wake of the structure and $H_{s,i}$ is the incident wave height. An illustration of the laboratory tests is presented in Figure 3.

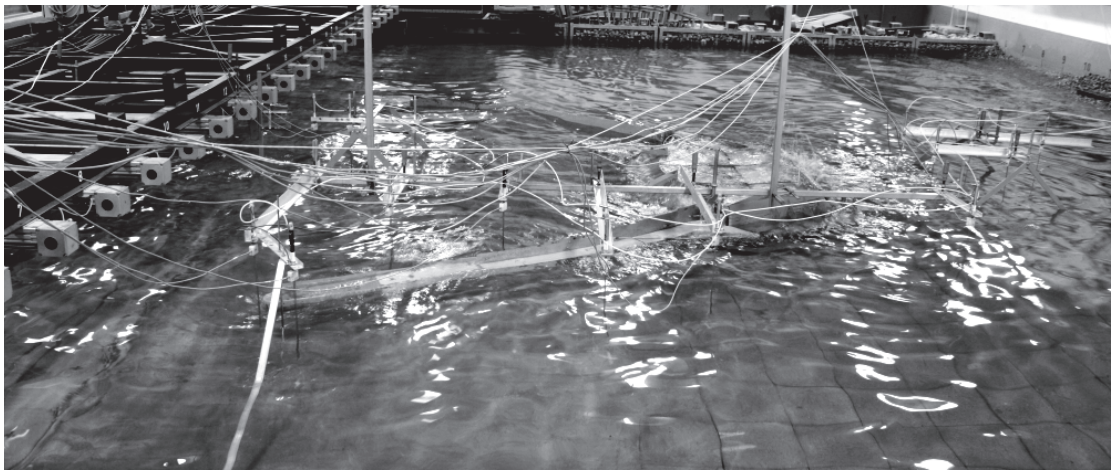

Figure 3. Photo from laboratory tests performed in the 3D laboratory basin at Aalborg University (Nørgaard et al., 2011).

The positioning of the wave gauges for determining wave disturbance coefficients is illustrated in Figure 4 together with the arrangement of the WD mooring system.

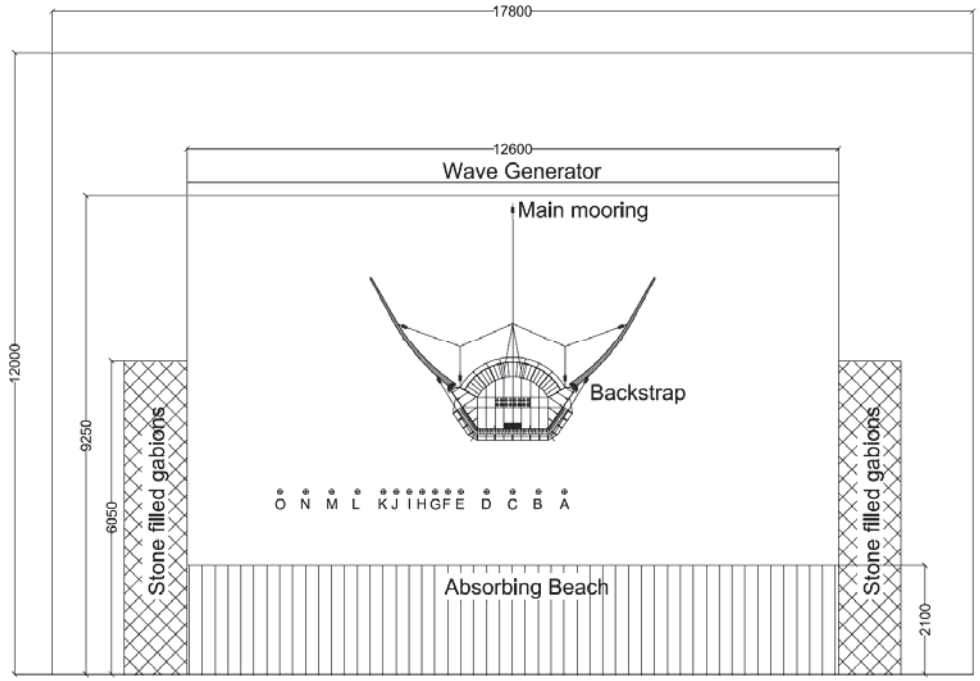

Figure 4. Positioning of wave gauges behind WD in laboratory basin. Dimensions are in *mm*. (Nørgaard et al., 2011)

Various irregular long crested JONSWAP wave spectra with γ = 3.3 and different stiffness in the main mooring lines were considered in the model tests by Nørgaard et al. (2011). The so-called

"normal"- and *"fixed"* mooring setups were evaluated in the study. In the *"normal"* setup the heave, surge, and pitch movements of the WD were controlled by applying springs in the mooring with pre-stress as recommended in Hald and Frigaard (2001). In the *"fixed"* mooring setup the WD was fixed in all its degree of freedom using vertically adjustable supports, which were bolted to the floor. The *"fixed"* mooring setup is not practical possible, but was evaluated by Nørgaard et al. (2011) as a reference, to determine the influence from the movements of the WD on the wave transmission characteristics.

From the tests by Nørgaard et al. (2011) it was concluded, that the wave transmission from the WD-device was more sensitive to the wave steepness, H_s/L_p, than to the crest freeboard rate, R_c/H_s (where R_c is the crest freeboard). Moreover, it was concluded that the mooring stiffness had a significant influence on the wave height reduction behind the WD.

It can thus be concluded that when modelling the wake effects from offshore floating WECs at a specific site it is especially important to simulate the different wave steepness present at the site and to simulate the correct stiffness of the mooring system.

The variation of the measured K_d by Nørgaard et al. (2011) in a line behind the WD is illustrated in Figure 5 for two different wave lengths. As seen from the figure, an almost parallel offset of the two fitted curves for the *"normal"* and the *"fixed"* mooring-setups is present for both considered wave-lengths.

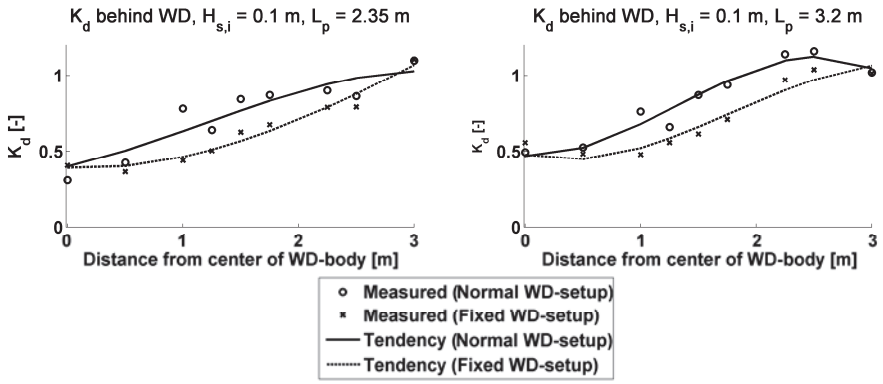

Figure 5. Wave disturbance measured along a line behind the WD. (Nørgaard & Andersen, 2012)

5. NUMERICAL WAVE PROPAGATION MODEL

The physical model tests by Nørgaard et al. (2011) were used by Nørgaard & Andersen (2012) for calibration of the commercial MIKE21 BW model by DHI. This model is further used for the case study in the present paper. The model is capable of reproducing combined effects of all important wave phenomena such as diffraction, refraction, shoaling, wave breaking, non-linear wave-wave interactions, and bottom dissipation. An extensive verification of the model is performed against both experimental and analytical data. The classical Boussinesq equations are limited to a maximum depth to deep-water wave length ratio of $h/L_0 \leq 0.22$, but so-called enhanced Boussinesq equations are introduced to extend the maximum depth to deep-water wave length ratio to $h/L_0 \leq 0.5$.

The MIKE21 BW model provide the opportunity to include porous structures, and the effects of non-Darcy flow through a porous media. In this way, it is possible in MIKE21 BW to simulate frequency dependent partial reflection, absorption and transmission of wave power. This is needed when simulating the frequency dependent wave transmission from a WD.

6. Previous Implementation of WD in MIKE21 Boussinesq

In Nørgaard & Andersen (2012) the WD was implemented in the model using porosity layers which were tuned to obtain the measured wave disturbance behind the device. The calibration was performed by varying the porosity layers through the structure to obtain the wanted transmission characteristics for the different considered wave lengths. The same approach was followed by Beels et al. (2010).

A regression analysis was performed by Nørgaard & Andersen (2012) between the modeled and measured wave disturbances. Moreover, the deviation between the measured and modeled transmitted wave power along the WD was determined using (1) where $P_{t,sim}$ is the simulated wave power and $P_{t,meas}$ is the measured wave power based on the measured H_s from the wave gauges. Results are shown in the figures.

$$P_{\text{t,diff.}} = \frac{\sum P_{\text{t,sim.}} - \sum P_{\text{t,meas.}}}{\sum P_{\text{t,meas.}}} \cdot 100\% \quad (1)$$

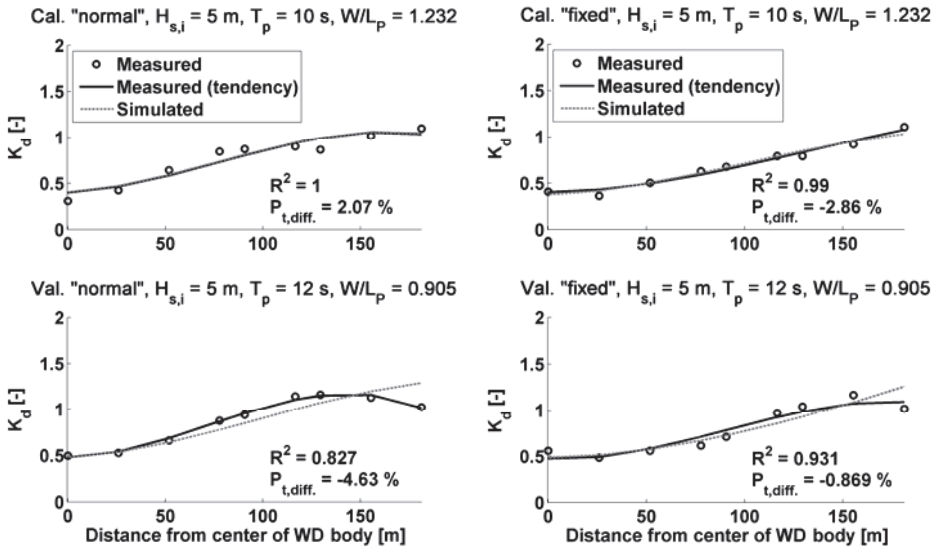

Figure 6. Implementation of "*normal*" and "*fixed*" WD-setup in MIKE21 BW. (Nørgaard & Andersen, 2012)

7. New Investigation of Overall Wave Transmission Coefficient from Multiple WDs in a Continuous Staggered Grid

Using the calibrated MIKE21 BW model the overall wave transmission of a farm of staggered WDs is determined for long and short crested waves using *"fixed"* and *"normal"* mooring-stiffness, shown in Figure 8. The continuous staggered grid of the WDs is illustrated in Figure 7. The wave transmission coefficient is defined as $K_t = \sqrt{p_t/p_i}$ where p_t and p_i are the transmitted and incident wave power, respectively. The approach of determining K_t from the numerical is further described in (Nørgaard & Andersen, 2012). Besides the wave-transmission obtained from the numerical model also the estimated K_t obtained from integration of wave flux (using 1. order wave theory) from the seabed to the draft of the WD is illustrated in Figure 8. The procedure of integration of wave flux is further described in (Nørgaard & Andersen, 2012).

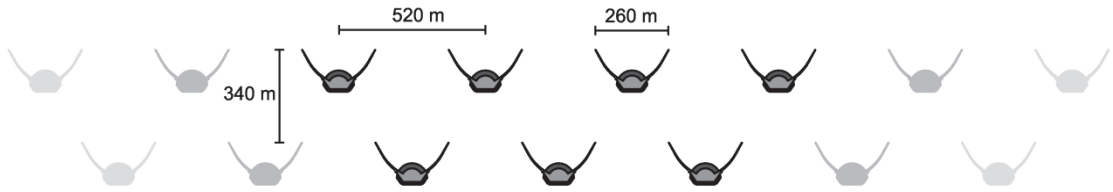

Figure 7. Positioning of WDs in a continuous staggered grid for determination of overall wave transmission coefficient.

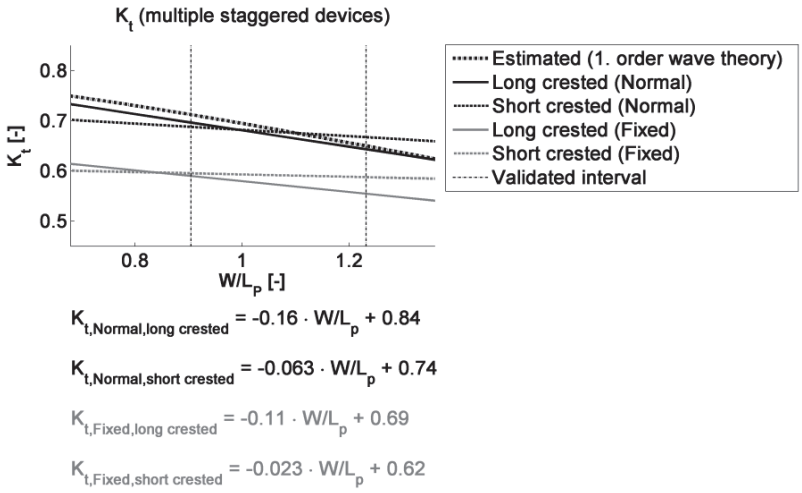

Figure 8. Overall wave transmission coefficient from a farm of staggered WDs.

As seen from Figure 8, the wave transmissions from long- and short crested waves are relatively similar. A significant reduction in K_t is found in the *"fixed"* WD setup compared to the realistic *"normal"* setup. The estimated K_t from the integration of wave flux is relatively close to the wave transmission from the *"normal"* setup and can be used as a good estimate instead of the detailed implementation of the WD based on physical model tests.

It should be mentioned, that the MIKE21 BW model is solely validated for long crested waves. However, since the model is capable of reproducing all important wave transformation phenomena, it is believed that a good estimate of K_t is obtained also in short crested waves.

8. SANTANDER BAY CASE STUDY SITE

Santander Bay is located on the Cantabrian coast of Spain - Gulf of Biscay, see Figure 9. The beaches of interest are a 2.5 *km* long sand spit, named El Puntal spit, and Magdalena beach, located at the peninsula north of the spit. The coast of Magdelena peninsula consists mainly of cliffs, while the spit consists of beaches and dunes of sand with a mean grain size along the spit of 0.3 *mm.*

Figure 9. Study site on the Cantabrian coast of Spain. Image is orientated to the north. (Google maps, 2011)

The evaluated wave conditions are given in Table 1. A typical winter-storm with H_s = 5 *m* is considered together with peak wave periods in the range T_p = 10 – 14 *s* (Medellín, 2008). T_p = 14 *s* (W/L_p = 0.749) is outside the validated range of W/L_p = 0.905 – 1.232 from model tests by Nørgaard et al. (2011) but the MIKE21 BW model is expected to provide a reasonable estimate also for this wave period.

Table 1. Considered wave conditions in numerical model of Santander bay.

Wave condition:	**1**	**2**	**3**
H_s [*m*]	5	5	5
T_p [*s*]	10	12	14
h [*m*]	25	25	25
W/L_p [-]	1.151	0.905	0.749

The waves in Santander bay are mostly approaching from north-west, i.e. long fetches from the North Atlantic Ocean. From Figure 10 it is seen, that especially the middle and eastern parts of the spit are fully exposed to the NW Cantabrian swell waves, which however, refract along the coast and turn into a more northerly direction.

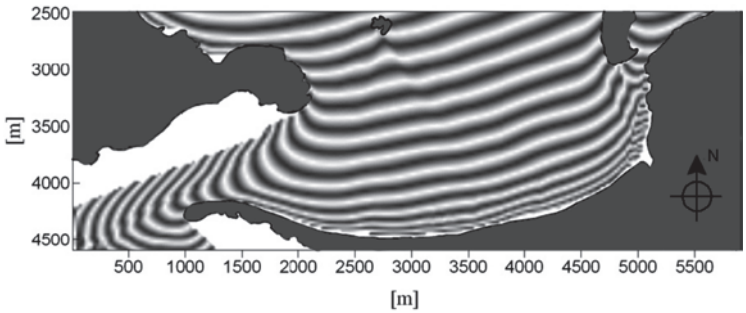

Figure 10. Wave propagation associated with typical storm wave conditions (H_s = 5 m, T_p = 16 s) from the NW-direction during high tide, performed by (GIOC, 2001).

In recent time, the morphology of El Puntal spit has been substantially modified. According to (Losada, 1991) approximately $2 \cdot 10^6$ m^3 of sand is lost along the spit in the past two centuries. Moreover, the Loredo region has retreated about 200 *m* (Losada, 1991). The present bathymetry of El Puntal spit is illustrated in Figure 11.

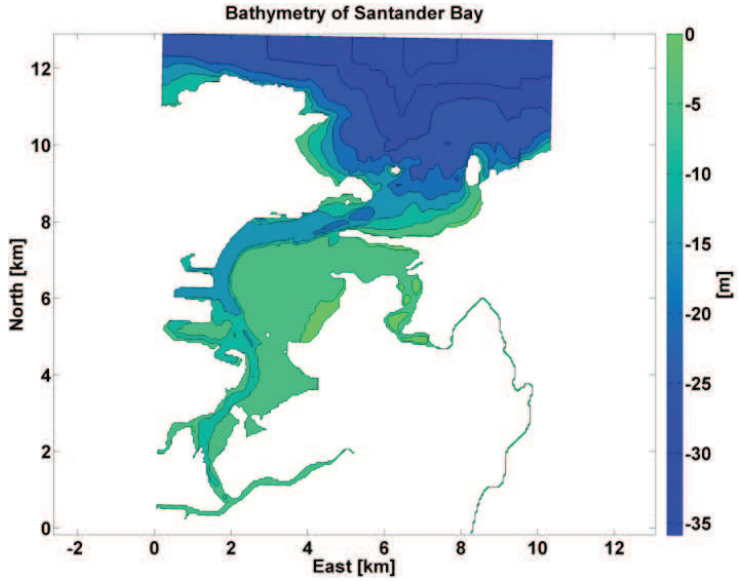

Figure 11. Present bathymetry of Santander Bay, Spain.

9. Implementation of Santander Bathymetry in MIKE21 BOUSSINESQ Study Site

The bathymetry of Santander Bay is implemented in MIKE21 BW by using bilinear interpolation between the contour lines in Figure 11. Since wave breaking at the shoreline is not of particular interest when simulating the wave disturbance, the minimum water depth at the beach is modified to avoid wave breaking (which can significantly increase the CPU-time). A minimum depth of h_{min} = 10 *m* is assumed, and thus shallower water-depths than h_{min} are replaced by a depth of 10 *m* in the bathymetry. The modified bathymetry is illustrated in Figure 12.

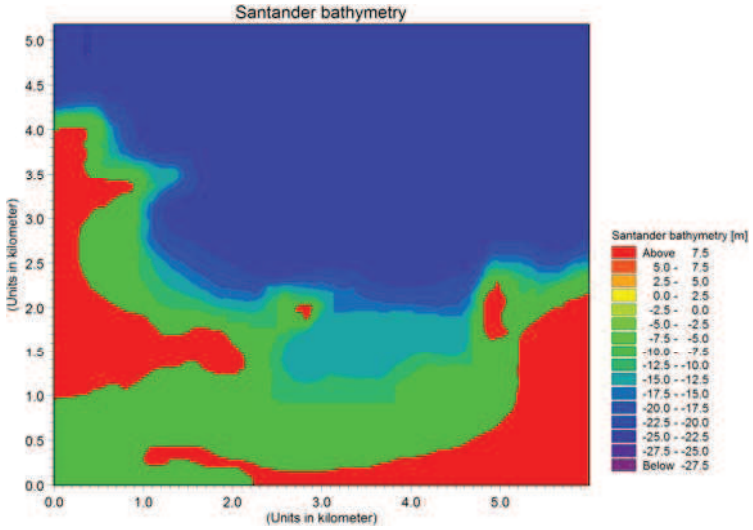

Figure 12. Modified bathymetry with the minimum water depth set to *h* = -10 *m*.

9.1 Modelling of Boundaries in Santander Bathymetry Study Site

No calibration of the wave climate in the bay is performed. However, the wave height reduction from the WDs in the bay is evaluated from a comparison between the situations with and without the presence of the WDs, and thus the influence from un-calibrated boundaries etc. is not expected to significantly influence the results.

As mentioned, the coastline of Santander consists of a mixture of sand beaches and cliff sides with different reflective properties. The beach areas are given a reflection coefficient of K_r = 0.1 (porosity value S = 0.96) with T_p = 10 s, while the areas with cliffs are given a reflection coefficient of K_r = 0.78 (porosity value S = 0.6). Open boundaries are modelled using sponge layers. The boundaries in the numerical model of Santander bay are illustrated in Figure 13 and summarized in Table 2.

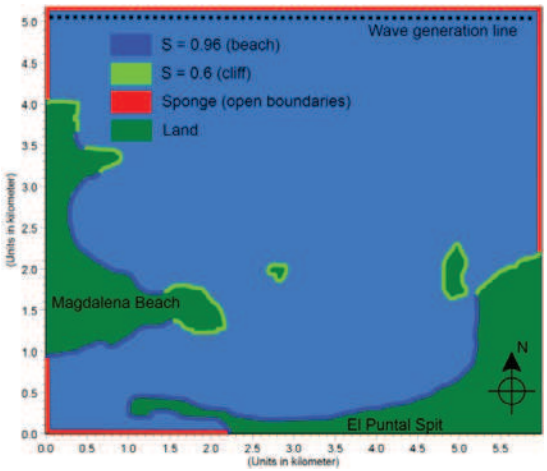

Figure 13. Porosity- and sponge layers for use in the numerical model of Santander bay.

Table 2. Specification of boundaries in model of Santander.

Boundary	Type, S	K_r (with T_p = 10 s)
Beach	0.96	0.1
Cliff	0.6	0.78
Open	Sponge	0

In Figure 10 it could be seen, that the most common wave direction is north-west some distance from the coast of Santander. However, it is observed, that the waves refracts, and turn towards a more northerly direction when approaching the entrance to Santander bay. Due to this, and to minimize the size of the computational domain, the study on wave height reduction behind WDs in Santander, is performed using waves approaching from north.

From a preliminary analysis, it is found that a minimum number of 1200 incident waves are required to obtain a converged model. Additionally, it is found that an element size of $dx = dy$ = 5.18 m is sufficient. Concerning the time discretization, a time step of dt = 0.15 s is chosen for the model, corresponding to a Courant number of 0.45.

9.2 Considered WD-Farm Layouts in Santander Bay Study Site

Beels et al. (2010) found that five WDs installed in a staggered grid with an individual distance of 2·B could produce five times the electricity of a single WD, whereas an individual distance of 1·B was seen to slightly reduce the power absorption in the second row.

In the present study two different staggered grids are considered, named "*Layout 1*" and "*Layout 2*" in the following. The two layouts are illustrated in Figure 14. Both considered WD-farm layouts are positioned approximately 4.5 *km* from the sand spit. "*Layout 1*" has a rated production of 76 *MW* and "*Layout* 2" has a rated production of 52 *MW*. A navigation channel for ship traffic is left open at the eastern corner upper of the bay. WDs in "*Layout* 1" and "*Layout* 2" are numbered according to Figure 14. The WD farms in "*Layout 1*" and "*Layout 2*" are both positioned at approximately 25 *m* water

depth, which was also the water depth used for calibration of the wave transmission coefficients in Figure 10.

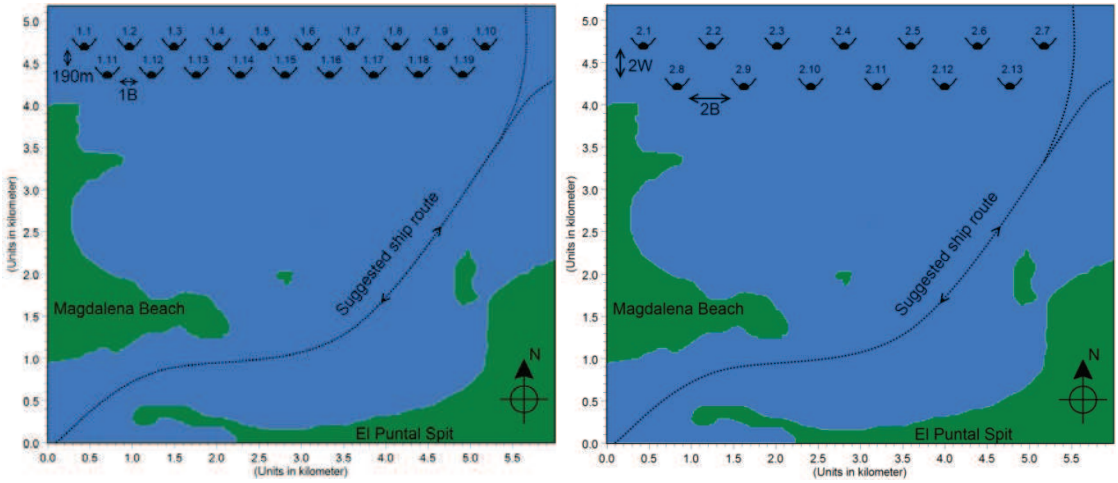

Figure 14. (*left*) Illustration of "*Layout 1*". (*right*) Illustration of "*Layout 2*".

10. Wave Height Reduction Behind Different WD-farm Layouts in Santander Bay Study Site

The effects from the different WD-farm layouts are compared along two output lines positioned in front of the sand spit, "*Output 1*", and in front of Magdalena Beach, "*Output 2*" c.f. Figure 15. The output lines are located just outside the wave breaking zone, since wave breaking is not included in the model. It should thus be noted, that the presented wave height reductions in the following are not the actual wave height reductions at the beach.

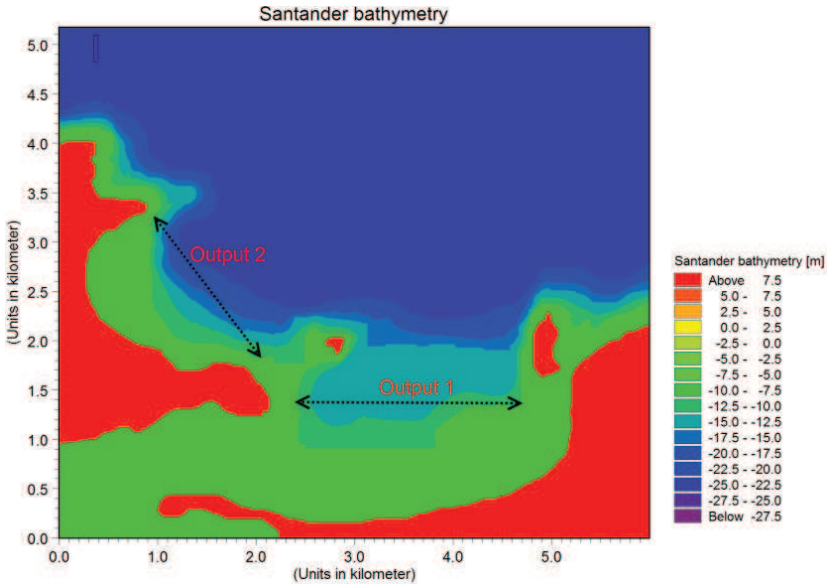

Figure 15. Illustration of output lines used for comparison of the wave height reduction from the different WD-farm layouts.

10.1 Evaluation of Wave Propagation without the Presence of WDs in Santander Bay

In Figure 16 the wave disturbance contours in the bay are illustrated in case of long- and short crested waves in absence of offshore WDs at the site.

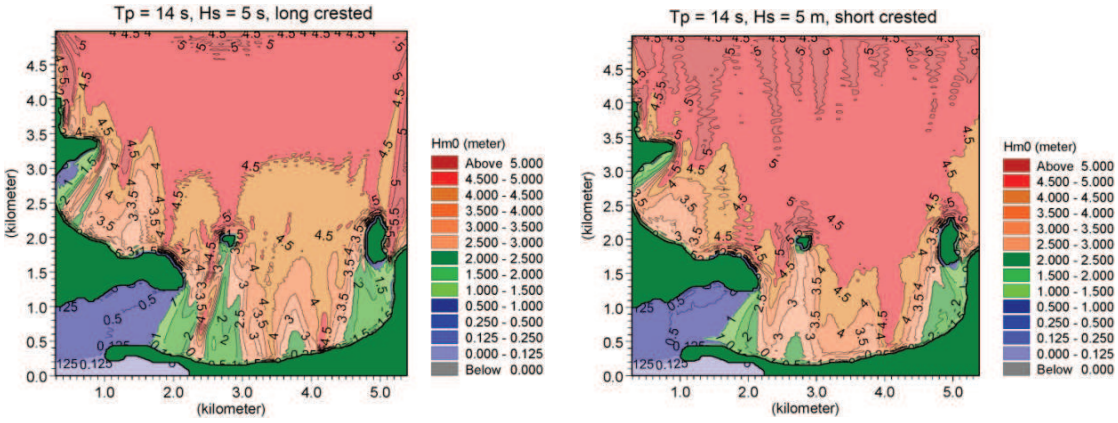

Figure 16. (*left*) H_{m0}-contours in case of long crested waves approaching from north. (*right*) H_{m0}-contours in case of short crested waves approaching from North.

As can be seen from Figure 16, the wave heights are reduced when approaching the coast due to refraction from the bottom contours. In the situation with long crested waves some diffraction is present in the western and eastern model boundaries due to the sponge layers. However, the diffraction contours are not entering the area of interest, and are thus not expected to have any effect on the results.

10.2 Wave Height Reduction from "Normal" and "Fixed WD-Setups and Influence from Wave Climate in Santander Bay Study Site

Both the *"normal"* and *"fixed"* WD-layouts are evaluated in order to obtain realistic and optimistic estimates of the wave transmissions. The wake effects from "*Layout 1*" in long- and short crested waves are illustrated in Figure 17.

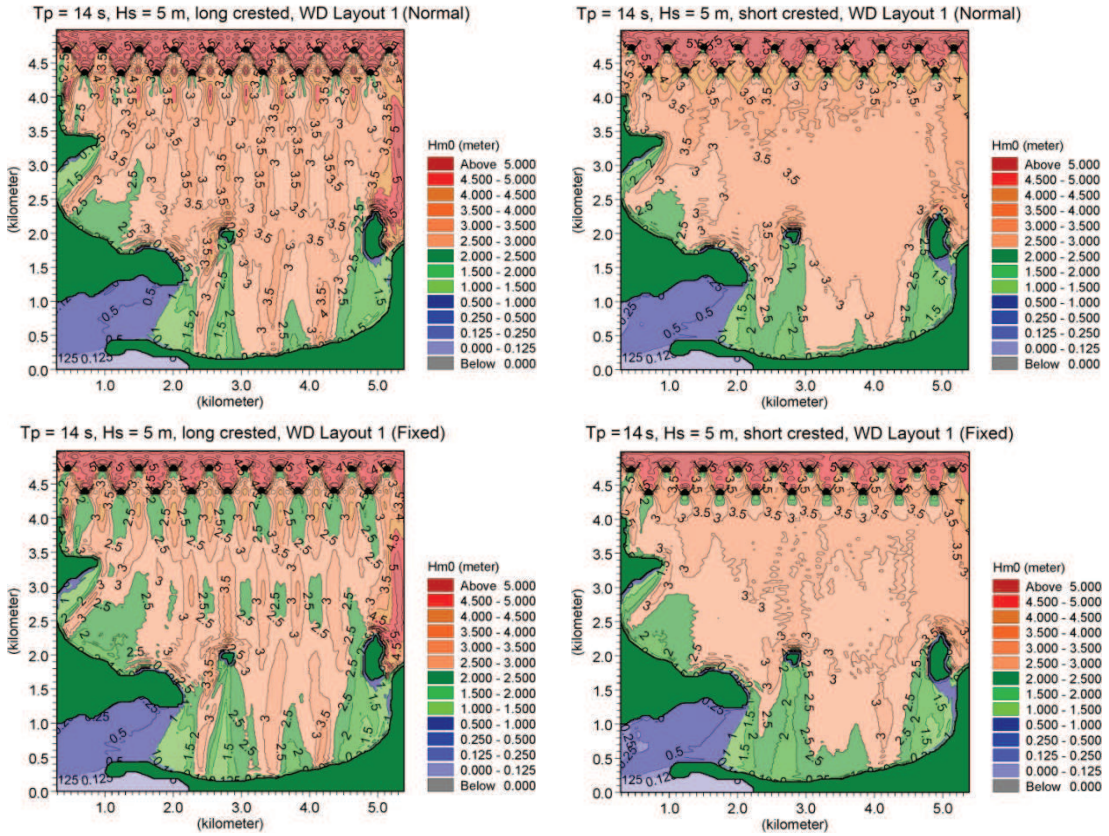

Figure 17. H_{m0}-contours for "*Layout 1*" in long- and short crested waves with the *"normal"* and *"fixed"* WD-setups.

As a comparable measure, the wake from the offshore WDs is described by the relative difference in transmitted wave power along the output lines obtained from (2). $P_{t,WD}$ is the transmitted wave power along the output lines in case of offshore positioned WDs and P_{normal} is the wave power along the output lines in case of *"normal"* conditions without WDs at the study site. Results are summarized in Figure 18.

$$P_{\text{t,diff.}} = \frac{\sum P_{\text{t,WD}} - \sum P_{\text{t,normal}}}{\sum P_{\text{normal}}} \cdot 100\% \qquad (2)$$

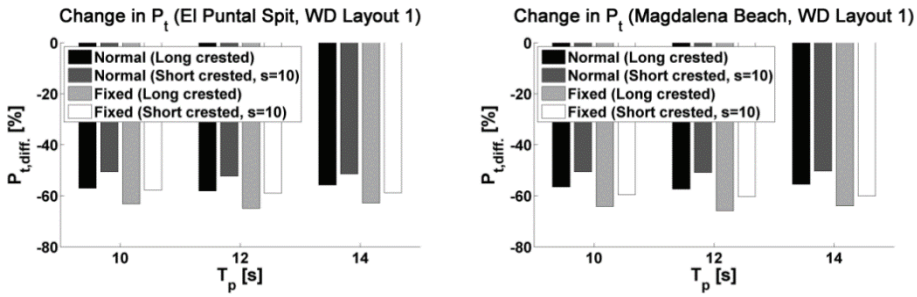

Figure 18. Relative difference in wave power for "*Layout 1*" along the output lines in case of *"normal"* and *"fixed"* WD-setups in long- and short crested waves.

As can be seen from Figure 18, the wave power along the output lines at El Puntal Spit and Magdalena Beach are reduced by approximately 60% compared to conditions without the presence of

the offshore WDs. A slightly bigger reduction in P_t is obtained for the *"fixed"* WD-setup compared to the *"normal"* setup. Moreover, a bigger reduction is obtained for long crested waves compared to short crested waves.

10.3 Comparison of WD-farm Layout 1 and 2 in Santander Bay Study Site

The wake effect from "*Layout 2*" in long- and short crested is illustrated in Figure 19. Only the *"normal"* WD-setup is considered.

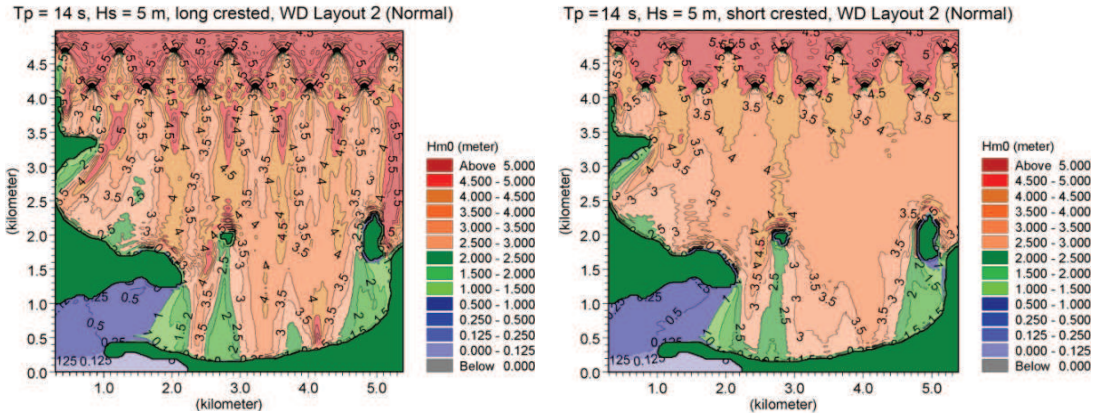

Figure 19. H_{m0}-contours for "*Layout 2*" in long- and short crested waves with the *"normal"* WD-setup.

The transmitted wave power from "*Layout 1*" and "*Layout 2*" is compared using (3). Results are summarized in Figure 20 for the "*normal*" and *"fixed"* WD-setup and in long crested and short crested waves. $P_{t,Layout\ 1}$ is the transmitted wave power along the output lines for "*Layout 1*" and $P_{t,Layout\ 2}$ $[W/m]$ is the transmitted wave power along the output lines for "*Layout 2*". As seen, more wave power is transmitted from "*Layout 2*" compared to "*Layout 1*". The difference in P_t is, however, slightly reduced for increasing T_p.

$$P_{\text{t,diff.}} = \frac{\sum P_{\text{t,Layout 1}} - \sum P_{\text{t,Layout 2}}}{\sum P_{\text{t,Layout 2}}} \cdot 100\% \qquad (3)$$

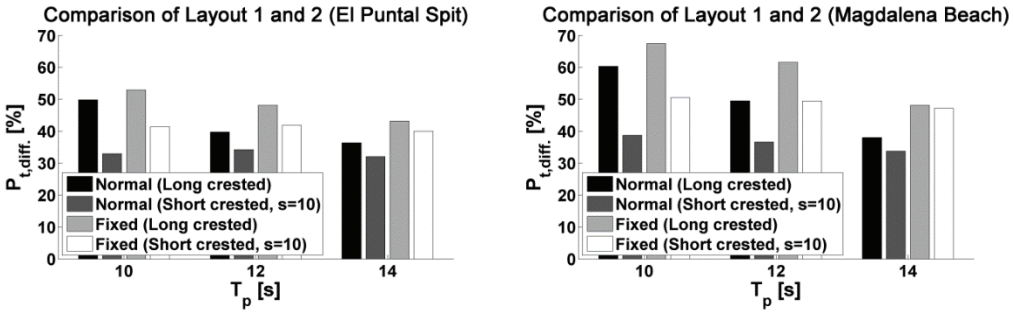

Figure 20. Relative difference in wave power along the output lines in case of *"normal"* and *"fixed"* WD-setups in long- and short crested waves.

The difference in incident wave power P_i between a WD in the first row compared to a WD in the second row is evaluated using (4), where $P_{i,First\ row}$ is the available wave power between the reflectors of a WD in the first row, and $P_{i,Second\ row}$ is the available wave power in the second row. Results are shown in Figure 21 where $WD_{1.5}$ and $WD_{1.15}$, c.f. Figure 14, are compared for "*Layout 1*" and $WD_{2.4}$ and $WD_{2.11}$ are compared for "*Layout 2*".

$$P_{\text{i,diff.}} = \frac{\sum P_{\text{i,First row}} - \sum P_{\text{i,Second row}}}{\sum P_{\text{i,Second row}}} \cdot 100\% \quad (4)$$

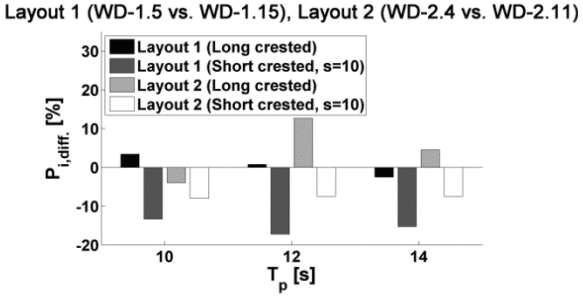

Figure 21. Relative difference in incident wave power between reflectors of WDs positioned in the first and second row for "*Layout 1*" and "*Layout 2*" in long crested and short crested waves and using the free WD setup.

As can be seen from Figure 21, $P_{i,Second\ row}$ is slightly increased in both evaluated farm layouts for long crested waves due to diffraction from the WDs in the first row. A relatively small difference in $P_{i,Second\ row}$ is observed between the two considered farm layouts. Thus, "*Layout 2*" is disregarded in further analysis since it has a relative large wave transmission, cf. Figure 20, and only a relatively small gain in absorbed wave power in the second row compared to "*Layout 1*", cf. Figure 21,.

10.4 Simplified Modelling of Wave Height Reduction from WDs in Santander Bay Study Site

Based on the overall wave transmission from the staggered WD farm in Figure 8 the wave height reduction in Santander bay can be modelled using a simplified homogeneous geometry of the WD farm instead of modelling the exact geometry of each WD. The implementation of a simplified geometry instead of modelling each single WD geometry in a farm, is illustrated in Figure 22.

Figure 22. Illustration of simplified modeling of wave transmission from a farm of staggered WDs based on overall wave transmission coefficients.

The wave height reduction behind the farm of WDs modelled using a staggered grid of WDs with exact geometry and modelled using a homogeneous geometry, are compared in Figure 23 along the output lines in Figure 15. The *"normal"* WD setup is evaluated, and both long and short crested waves are considered in the figure. As seen, especially in case of short crested waves the wave heights along the output lines are very similar.

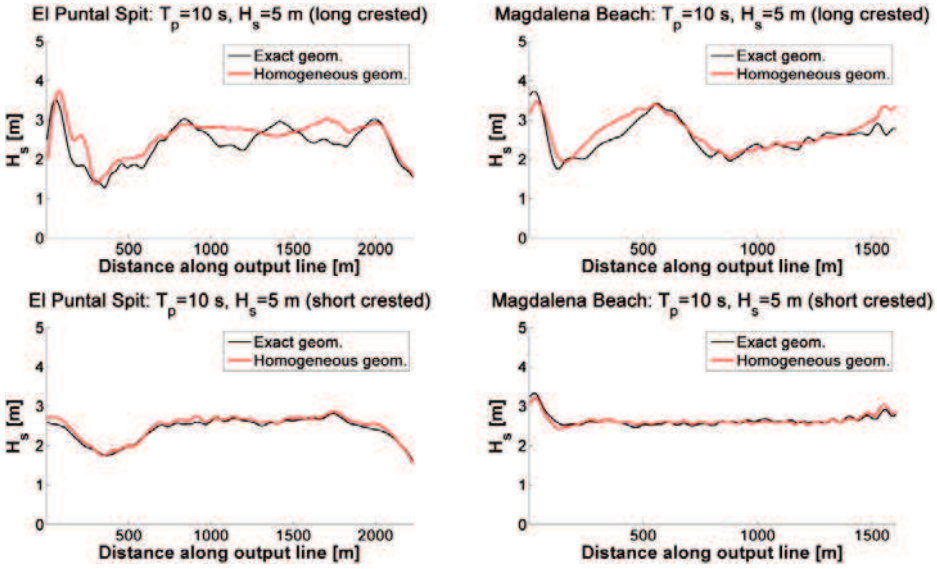

Figure 23. Wave height reduction behind from exact WD geometry and homogeneous simplified WD geometry.

The difference in transmitted wave power at Magdalena beach and at Santander Spit from a farm of WDs modeled with correct geometries, $P_{t,Exact}$, and a homogeneous geometry, $P_{t,homogeneous}$, is determined using (5). Results are illustrated in Figure 24. The porosity of the homogeneous geometry is based on K_t in Figure 8 for T_p = 10 *s* and unchanged for the other considered wave periods.

$$P_{\text{t,diff.}} = \frac{\sum P_{\text{t,Homogeneous}} - \sum P_{\text{i,Exact}}}{\sum P_{\text{i,Exact}}} \cdot 100\% \qquad (5)$$

As can be seen from Figure 24, the biggest difference between the exact and homogeneous geometries is found for long crested waves. The homogeneous geometry is slightly overestimating the transmitted wave power along both output lines for T_p = 10 *s* but the difference become smaller for increasing wave periods.

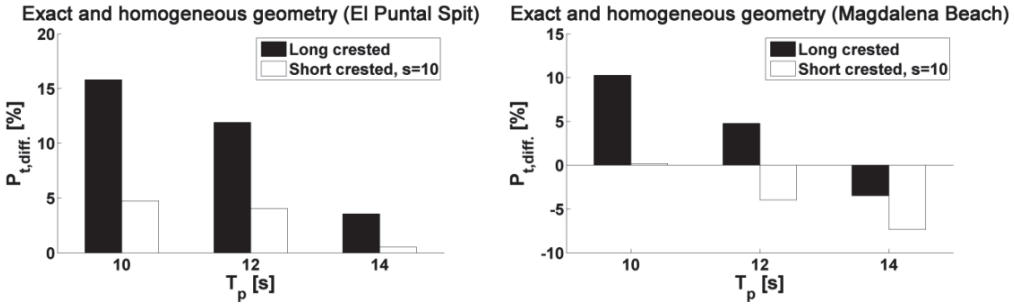

Figure 24. Difference in transmitted wave power at Magdalena beach and at Santander Spit from the exact WD geometry and homogeneous WD farm geometry.

11. CONCLUSIONS

The objective of the present paper has been to obtain a realistic estimate of the wave height reduction behind floating Wave Dragon wave energy converters in Santander Bay, Spain.

The MIKE21 BW model was used in the study, which was previously calibrated by Nørgaard & Lykke Andersen (2012) against the physical model tests by Nørgaard et al. (2011). The implementation

of the WD in the numerical model was performed using so-called porosity layers. Using the calibrated model an overall wave transmission coefficient was determined from a farm of staggered WDs in various wave conditions. A realistic wave transmission coefficient of approximately K_t = 0.7 was obtained for peak wave periods around T_p = 10 – 14 *s* (decreasing for higher T_p).

Two different farm layouts; *"Layout 1*" and "*Layout 2*" with two different individual distances between the staggered devices were evaluated; one WD-width and two WD widths, respectively. Both farms were positioned approximately 4.5 *km* from the sand spit in Santander Bay. "*Layout 2*" was concluded by Beels et al. (2010) to be optimal in terms of electricity production, since devices in the second row were unaffected by diffraction from the devices in the first row. However, "*Layout 1*" was concluded in the present study to be the best compromise between electricity production and coastal protection since the devices in the first and second row were overlapping and thus no area was left unprotected behind the farm. The difference in electricity production between "*Layout 1*" and "*Layout 2*" was relatively small. A realistic estimate of the wave power reduction behind "*Layout 1*" was around 55% in Santander Bay, Spain, using the "*normal*" mooring setup.

Instead of implementing the detailed geometries of the WDs in the numerical wave propagation model, a simplified implementation can be performed by calculating the overall wave transmission coefficient of the farm using integration of wave power below the floating devices, and thereby model the farm using a complete homogeneous structure.

12. Discussion

From the findings in the present paper it is seen, that there is a great potential in using wave energy converters as multi-functioning coastal protection structures. Expected future climate changes introduce an increasing need for upgrading existing coastal defences and combined wave energy converters and breakwaters may be good green alternatives to other upgrade possibilities. Moreover, shared costs between coastal protection and electricity production may help introducing new wave energy devices, which are able to compete with other renewable energy sources.

13. Acknowledgements

The support of the European Commission through FP7.2009-1, Contract 244104 - THESEUS ("Innovative technologies for safer European coasts in a changing climate"), is gratefully acknowledged.